Effect of Dispersion of Inorganic Nanoparticles on the Phase Behavior of Block Copolymers in a Selective Solvent

Chieh-Tsung Lo,[†] Byeongdu Lee,[†] Randall E. Winans,[†,‡] and P. Thiyagarajan*[,§]

X-ray Science Division, Chemistry Division, and Intense Pulsed Neutron Source, Argonne National Laboratory, 9700 S. Cass Ave., Argonne, Illinois 60439

Received April 19, 2006
Revised Manuscript Received July 6, 2006

Introduction. Controlled ordering of nanoparticles in block polymer matrices has been exploited to synthesize novel composites for a variety of applications such as catalysis, semiconductors, photonic materials, electricity, and biological and medical fields.[1−3] Recently, a novel strategy[4−7] has been developed to organize nanoparticles in polymer matrices with controlled patterns by exploiting microphase separation of block copolymers, and it is observed that the confinement of nanoparticles in organized patterns improves the optical[8,9] and mechanical properties[10] of the nanocomposites. To gain better insight into the physical properties of these functional materials, significant effort is being devoted to understanding the morphologies of nanocomposites both theoretically and experimentally.[11−15]

Since solvent selectivity is an important parameter that determines the phase behavior of block copolymer solutions,[16−19] its role has to be considered in solution-based synthetic routes for tailoring morphologies of nanocomposites. It has been found that order−disorder (ODT) and order−order (OOT) transition temperatures are correlated to the polymer concentration in solution, and the composition profiles and dimensions of microdomains vary with dilution.[19−21] In a selective solvent, the solvent expands only the favorable block, causing shifts along both temperature and composition directions in the phase diagram. Effects similar to this can also be obtained by sequestering nanoparticles in the favorable domain. By using solvents with different selectivity and concentration of polymer and nanoparticles, it would be possible to tune the morphologies in the microdomains and consequently the nanocomposites.

In this Communication, we report the phase behavior of PS−PVP copolymers in a selective solvent as a function of temperature and concentration of nanoparticles using SANS. In contrast to X-ray scattering (SAXS) in which gold nanoparticles dominate the scattering signal and swamp the contribution from copolymers, SANS of samples in deuterated solvents provide good contrast for the scattering from copolymers. Our goal is to understand how the loading of nanoparticles affects the phase behavior of block copolymers in solvents, and this information will be useful in the processing of bulk nanocomposites.

Experimental Section. We followed established procedures for the synthesis of Au nanoparticles[22] and polymer nanocomposites.[7] Briefly, hydrogen tetrachloroaureate(III) trihydrate (Aldrich Chemical Co., Inc.) and thiol-terminated PS (M_n = 1500 g/mol, PDI = 1.10, Polymer Source, Inc.) with a molar ratio of 1 were mixed in THF (≥99.9%, Aldrich Chemical Co., Inc.). A 1.0 M lithium triethylborohydride in THF (Aldrich Chemical Co., Inc.) was added dropwise to reduce Au ions to nanoparticles. The nanoparticles were purified using methanol (≥99.8%, Aldrich Chemical Co., Inc.) to remove the residual ions and unbound thiol groups. SAXS showed that the purified nanoparticles in THF have a diameter ∼3.6 nm.[23] To prepare nanoparticle/copolymer complexes in solution, Au nanoparticles with thiol-terminated PS was mixed with PS−PVP (M_n = 96 800, f_{PS} = 0.57, PDI = 1.04, Polymer Source, Inc.) in *d*-toluene (99.6% D, Aldrich Chemical Co., Inc.), which is selective to PS but nonselective to PVP.

SANS experiments were performed on samples sealed in 1 mm path length quartz cells using the time-of-flight SAND instrument at the Intense Pulsed Neutron Source at Argonne National Laboratory. Data were collected and reduced in the Q [$(4\pi/\lambda)$ sin θ, θ is half the scattering angle and λ is the wavelength] range of 0.004−0.3 Å^{-1}. Correction for the background from the empty cell, parasitic scattering, and absorption was carried out following routine procedures.

Results and Discussion. Figure 1 shows SANS data of neat PS−PVP (volume fraction = 34.2%) and its complexes with PS-grafted Au nanoparticles (here after referred to as PS−PVP/Au) in *d*-toluene as a function of temperature. For the neat polymer solution at low temperatures (Figure 1a), distinct peaks are observed in the SANS data at Q^* (first-order peak position) values with a ratio of 1:$\sqrt{7}$, suggesting that the system has hexagonally packed cylindrical structure. The intermediate order peaks are missing presumably due to less ordered nature of the polymer in solution. Since toluene is a good solvent for PS, but a poor solvent for PVP, it swells the PS domains in the ordered microstructure, leading to a transformation from the preferred lamellar in the bulk to a cylindrical morphology. At higher temperatures the molecular repulsion between PS and PVP decreases due to the upper critical solution temperature behavior of PS−PVP.[24] Consequently, this decreases the solvent selectivity for the PS domain, causing the solvent to distribute in the PVP domain which progressively reduces the interfacial curvature with increasing temperature. At 70 °C an order−order transition occurs, and the copolymer solution exhibits a lamellar structure (Figure 1a). This picture is consistent with the phase behavior of poly(styrene-*b*-isoprene) in solvents with different selectivity.[17,19,20,25,26]

In the neat copolymer solution, the phase behavior is governed by the polymer/polymer and polymer/solvent interactions. On the other hand, in the PS−PVP/Au complex solution an additional long-range interaction due to the presence of nanoparticles in PS domains arises. The thermodynamic equilibrium in this solution, therefore, is governed by the balance between the interactions between the PS and PVP blocks and their interaction with the solvent and the confined nanoparticles. Figure 1b shows the SANS data of 34.2% PS−PVP/Au complex [$\phi_{PS-PVP/Au} = (V_{PS-PVP} + V_{Au})/(V_{PS-PVP} + V_{Au} + V_{toluene}) \times 100\%$, assuming additivity of volumes, where $\phi_{PS-PVP/Au}$ is the volume fraction of PS−PVP/Au complex in *d*-toluene and V_{PS-PVP}, V_{Au}, and $V_{toluene}$ are the volumes of PS−PVP, PS-grafted Au nanoparticles, and *d*-toluene, respectively] with 17.9% Au nanoparticles [$\phi_{Au} = V_{Au}/(V_{PS-PVP} + V_{Au}) \times 100\%$, where ϕ_{Au} is the volume fraction of Au nanoparticles in the PS−PVP/Au complex] in *d*-toluene. The confinement of nano-

[†] Experimental Facilities Division.
[‡] Chemistry Division.
[§] Intense Pulsed Neutron Source.
* To whom all correspondence should be addressed: e-mail: thiyaga@anl.gov.

10.1021/ma060879o CCC: $33.50
Published on Web 08/16/2006

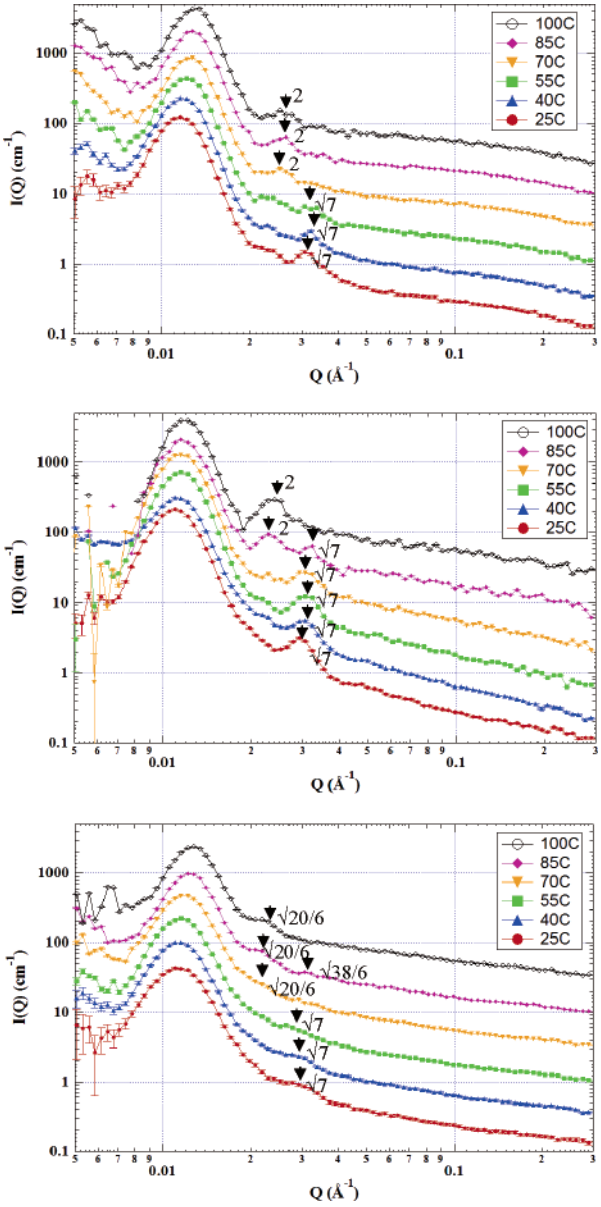

Figure 1. SANS profiles of (a) neat and PS−PVP complexes with (b) ϕ_{Au} = 17.9% and (c) ϕ_{Au} = 36.8% nanoparticle in *d*-toluene ($\phi_{PS-PVP/Au}$ = 34.2%) as a function of temperature. (Scattering patterns have been shifted to increase clarity, and the arrows and numbers in the plots show ratio of the peak positions to the Q^* value of the first-order peak.)

particles causes swelling of the PS domains, reminiscent of the behavior of the selective solvents. However, with increasing temperature while the solvent distributes to PVP domain the nanoparticles will remain confined to the PS domain presumably due to entanglement. Consequently, this limits the changes in the overall interfacial curvature during the distribution of the solvent, causing slow transitions in the block copolymer phase behavior. While a transition between cylindrical to lamellar morphology occurs between 55 and 70 °C for the neat polymer solution (Figure 1a), we observe a cylindrical structure at 70 °C for the PS−PVP/Au solution, a coexistence of lamellar and cylindrical structures at 85 °C, and a complete phase transformation to lamellar structure at 100 °C (Figure 1b). It should be noted that the data below 85 °C show only weak peaks at $\sqrt{4}Q^*$ that correspond to the cylindrical microstructure. At 36.8% Au a different phase behavior occurs as shown in Figure 1c. Depending on the concentration of the confined nanoparticles

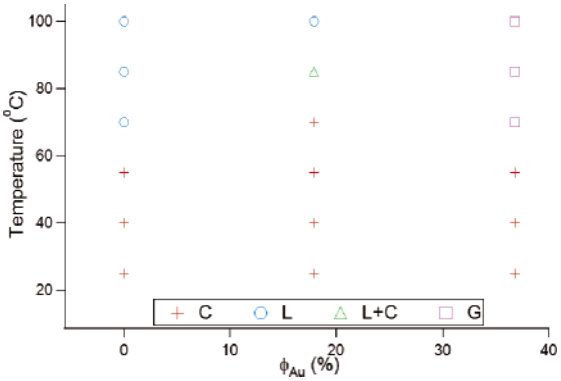

Figure 2. Phase diagram of PS−PVP in toluene as a function of temperature and nanoparticle concentration. L, C, and G denote lamellar, cylindrical, and gyroid microphases.

the rate of the temperature-dependent transitions to different morphologies is affected. The higher the concentration, the slower the rate is. At this particle concentration, an order−order transition appears to occur from cylindrical to gyroid structure at 70 °C and the gyroid structure retains even at 100 °C. Interestingly, with increasing particle concentration, the phase behavior of the PS−PVP/Au complex in solution exhibits cylindrical→ gyroid transition at 70 °C (Figure 2) that differs from the order in the sequence of phase transitions of bulk block copolymers from lamellar → gyroid → cylindrical → spherical structures with increasing volume fraction of one block. It has to be pointed out that the solvent and the grafted nanoparticles compete for the available space in the PS domain. Although both nanoparticles and solvent partition into the PS domain, solvent cannot swell the nanoparticles whose presence effectively decreases the swelling volume. At relatively higher nanoparticle loading, when the available volume in the PS domain is filled within the limits of the packing constraints, the excess solvent might be pushed either to the PS−PVP interface or to the PVP domain. Consequently, the rate of change of interfacial curvature might be significantly altered, and the system shows cylindrical→ gyroid transition. At high nanoparticle loading they screen the long-range order in the complex, causing the microdomains to spatially disorder.[14,23,27] With the addition of nanoparticles, the higher order peaks corresponding to the gyroid phase become broader and weaker.

Conclusions. We investigated the phase behavior of block copolymer and polymer/nanoparticle complexes in a selective solvent using SANS. The morphology of both polymer and complex solutions shows a strong function of temperature. This behavior is consistent with the fact that the selective solvent swells the preferred domain of the block copolymer causing phase transformations. As temperature increases, the repulsive interaction between the PS and PVP reduces, weakening the interfacial tension. Comparison of the phase behavior of neat and nanoparticle loaded copolymer solutions (Figure 2) shows pronounced variations in the resulting morphologies. When nanoparticles are sequestered in one domain, they swell that domain and increase the interfacial curvature, causing the changes in the morphology of the copolymer/nanoparticle complex. In contrast to the solvent, the inability of the nanoparticles to readily diffuse out of the favorable domain at elevated temperatures constrains the interfacial curvature, causing slow transitions in the block copolymer phase behavior.

To our knowledge this is the first experimental study on the phase behavior of block copolymer/nanoparticle complexes in solution. A dramatic effect of nanoparticles on the phase diagram of PS−PVP/Au in a selective solvent was found. Detailed

investigations of nanocomposites with respect to the volume fraction of nanoparticles and molecular properties of copolymers in both selective and neutral solvents are underway.

Acknowledgment. This work was supported by the LDRD Project No. 2005-219-N0 and benefited by the use of APS and IPNS funded by DOE-BES under Contract #W-31-109-ENG-38. We acknowledge D. G. Wozniak for his assistance in SANS experiments.

References and Notes

(1) Hamley, I. W. *Angew. Chem., Int. Ed.* **2003**, *42*, 1692−1712.
(2) Shenhar, R.; Norsten, T. B.; Rotello, V. M. *Adv. Mater.* **2005**, *17*, 657−669.
(3) Bockstaller, M. R.; Mickiewicz, R. A.; Thomas, E. L. *Adv. Mater.* **2005**, *17*, 1331−1349.
(4) Tsutsumi, K.; Funaki, Y.; Hirokawa, Y.; Hashimoto, T. *Langmuir* **1999**, *15*, 5200−5203.
(5) Bockstaller, M. R.; Lapetnikov, Y.; Margel, S. Thomas, E. L. *J. Am. Chem. Soc.* **2003**, *125*, 5276−5277.
(6) Sohn, B.-H.; Choi, J.-M.; Yoo, S. I.; Yun, S.-H.; Zin, W.-C.; Jung, J. C.; Kanehara, M. Hirata, T.; Teranishi, T. *J. Am. Chem. Soc.* **2003**, *125*, 6368−6369.
(7) Chiu, J. J.; Kim, B. J.; Kramer, E. J.; Pine, D. J. *J. Am. Chem. Soc.* **2005**, *127*, 5036−5037.
(8) Buxton, G. A.; Lee, J. Y.; Balazs, A. C. *Macromolecules* **2003**, *36*, 9631−9637.
(9) Bockstaller, M. R.; Thomas; E. L. *Phys. Rev. Lett.* **2004**, *93*, 166106.
(10) Buxton, G. A.; Balazs, A. C. *Phys. Rev. E* **2003**, *67*, 031802.
(11) Thompson, R. B.; Ginzburg, V. V.; Matsen, M. W.; Balazs, A. C. *Science* **2001**, *292*, 2469−2472.
(12) Thompson, R. B.; Ginzburg, V. V.; Matsen, M. W.; Balazs, A. C. *Macromolecules* **2002**, *35*, 1060−1071.
(13) Lee, J. Y.; Thompson, R. B.; Jasnow, D.; Balazs, A. C. *Macromolecules* **2002**, *35*, 4855−4858.
(14) Schultz, A. J.; Hall, C. K.; Genzer, J. *Macromolecules* **2005**, *38*, 3007−3016.
(15) Lin, Y.; Boker, A.; He, J.; Sill, K.; Xiang, H.; Abetz, C.; Li, X.; Wang, J.; Emrick, T.; Long, S.; Wang, Q.; Balazs, A.; Russell, T. P. *Nature (London)* **2005**, *434*, 55−59.
(16) Shibayama, M.; Hashimoto, T.; Kawai, H. *Macromolecules* **1983**, *16*, 16−28.
(17) Hamley, I. W.; Fairclough, J. P.; Ryan, A. J.; Ryu, C. Y.; Lodge, T. P.; Gleeson, A. J.; Pedersen, J. S. *Macromolecules* **1998**, *31*, 1188−1196.
(18) Hanley, K. J.; Lodge, T. P. *J. Polym. Sci., Polym. Phys. Ed.* **1998**, *36*, 3101−3113.
(19) Lodge, T. P.; Pudil, B.; Hanley, K. J. *Macromolecules* **2002**, *35*, 4707−4717.
(20) Hanley, K. J.; Lodge, T. P.; Huang, C.-I. *Macromolecules* **2000**, *33*, 5918−5931.
(21) Lodge, T. P.; Hanley, K. J.; Pudil, B.; Alahapperuma, V. *Macromolecules* **2003**, *36*, 816−822.
(22) Yee, C. K.; Jordan, R.; Ulman, A.; White, H.; King, A.; Rafailovich, M.; Sokolov, J. *Langmuir* **1999**, *15*, 3486-3491.
(23) Lo, C.-T.; Lee, B.; Dietz, N. L.; Winans, R. E.; Thiyagarajan, P., manuscript in preparation.
(24) Schulz, M. F.; Khandpur, A. K.; Bates, F. S.; Almdal, K.; Mortensen, K.; Hajduk, D. A.; Gruner, S. M. *Macromolecules* **1996**, *29*, 2857−2867.
(25) Huang, C.-I.; Lodge, T. P. *Macromolecules* **1998**, *31*, 3556−3565.
(26) Lai, C.; Russel, W. B.; Register, R. A. *Macromolecules* **2002**, *35*, 841−849.
(27) Huh, J.; Ginzburg, V. V.; Balazs, A. C. *Macromolecules* **2000**, *33*, 8085−8096.

MA060879O